6p25 in those two patients might influence the function of *FOXC1* and other neighboring genes because most patients with simple *FOXC1* mutations had only intraocular abnormalities. The array of *FOXC1* mutations with which clinical phenotype are documented is shown in Figure 5 [Mears et al., 1998; Nishimura et al., 1998, 2001; Swiderski et al., 1999; Mirzayans et al., 2000; Kawase et al., 2001; Suzuki et al., 2001]. Of the 70 patients with documented *FOXC1* mutations, 8 patients had hypertelorism, and 7 had cardiac anomalies. These two phenotypes may be relatively frequent in patients with *FOXC1* mutations. In contrast, dental and umbilical defects were frequently observed in ARA patients with *PITX2* mutations, and hypertelorism and cardiac anomalies were rarely seen in these patients [Semina et al., 1996b; Schinzel et al., 1997; Alward et al., 1998; Flomen et al., 1998; Kulak et al., 1998; Doward et al., 1999; Perveen et al., 2000; Priston et al., 2001; Saadi et al., 2001; Semina, 2004]. Although actual frequencies of extraocular dysmorphic features associated with of Rieger syndrome have not been established, umbilical and dental anomalies seem to accompany *PITX2* defects frequently, while hypertelorism and cardiac anomalies are often associated with *FOXC1* defects. This difference in the spectrum of extraocular phenotypes between *FOXC1* and *PITX2* lesions could be due to differences in tissue-specific expression of *PITX2* versus *FOXC1* [Semina et al., 1996b; Nishimura et al., 1998].

Understanding the relationship between the genetic lesions and clinical manifestations in patients with Axenfeld–Rieger syndrome would provide better clinical management and genetic evaluation, but this relationship is a complex and difficult matter. Further studies on the function(s) of two genes, *FOXC1* and *PITX2*, or other unrecognized genes in the 6p25 region are necessary.

REFERENCES

Alward WL. 2000. Axenfeld–Rieger syndrome in the age of molecular genetics. Am J Ophthalmol 130:107–115.

Alward WL, Semina EV, Kalenak JW, Héon E, Sheth BP, Stone EM, Murray JC. 1998. Autosomal dominant iris hypoplasia is caused by a mutation in the Rieger syndrome (RIEG/PITX2) gene. Am J Ophthalmol 125:98–100.

Anderlid BM, Schoumans J, Hallqvist A, Stahl Y, Wallin A, Blenow E, Nordenskjold M. 2003. Cryptic subtelomeric 6p deletion in a girl with congenital malformations and severe language impairment. Eur J Hum Genet 11:89–92.

Baruch AC, Erickson R. 2001. Axenfeld–Rieger anomaly, hypertelorism, clinodactyly, and cardiac anomalies in sibs with an unbalanced translocation der(6)t(6;8). Am J Med Genet 100:187–190.

Doward W, Perveen R, Lloyd IC, Ridgway AE, Wilson L, Black GC. 1999. A mutation in the RIEG1 gene associated with Peters' anomaly. J Med Genet 36:152–155.

Fitch N, Kaback M. 1978. The Axenfeld syndrome and the Rieger syndrome. J Med Genet 15:30–34.

Flomen RH, Vatcheva R, Gorman PA, Baptista PR, Groet J, Barisić I, Ligutic I, Nizetić D. 1998. Construction and analysis of a sequence-ready map in 4q25: Rieger syndrome can be caused by haploinsufficiency of RIEG, but also by chromosome breaks approximately 90 kb upstream of this gene. Genomics 47:409–413.

Gould DB, Jaafar MS, Addison MK, Munier F, Ritch R, MacDonald IM, Walter MA. 2004. Phenotypic and molecular assessment of seven patients with 6p25 deletion syndrome: Relevance to ocular dysgenesis and hearing impairment. BMC Med Genet 5:17.

Kawase C, Kawase K, Taniguchi T, Sugiyama K, Yamamoto T, Kitazawa Y, Alward WL, Stone EM, Nishimura DY, Sheffield VC. 2001. Screening for mutations of Axenfeld–Rieger syndrome caused by FOXC1 gene in Japanese patients. J Glaucoma 10:477–482.

Kulak SC, Kozlowski K, Semina EV, Pearce WG, Walter MA. 1998. Mutation in the RIEG1 gene in patients with iridogoniodysgenesis syndrome. Hum Mol Genet 7:1113–1117.

Kume T, Deng KY, Winfrey V, Gould DB, Walter MA, Hogan BL. 1998. The forkhead/winged helix gene Mfl is disrupted in the pleiotropic mouse mutation congenital hydrocephalus. Cell 93:985–996.

Law CJ, Fisher AM, Temple IK. 1998. Distal 6p deletion syndrome: A report of a case with anterior chamber eye anomaly and review of published reports. J Med Genet 35:685–689.

Lehmann OJ, Ebenezer ND, Ekong R, Ocaka L, Mungall AJ, Fraser S, McGill JI, Hitchings RA, Khaw PT, Sowden JC, Povey S, Walter MA, Bhattacharya SS, Jordan T. 2002. Ocular developmental abnormalities and glaucoma associated with interstitial 6p25 duplications and deletions. Invest Ophthalmol Vis Sci 43:1843–1849.

Lin RJ, Cherry AM, Chen KC, Lyons M, Hoyme HE, Hudgins L. 2005. Terminal deletion of 6p results in a recognizable phenotype. Am J Med Genet Part A 136A:162–168.

Lines MA, Kozlowski K, Walter MA. 2002. Molecular genetics of Axenfeld–Rieger malformations. Hum Mol Genet 11:1177–1184.

Maclean K, Smith J, St Heaps L, Chia N, Williams R, Peters GB, Onikul E, McCrossin T, Lehmann OJ, Adès LC. 2005. Axenfeld–Rieger malformation and distinctive facial features: Clues to a recognizable 6p25 microdeletion syndrome. Am J Med Genet Part A 132A:381–385.

Martinet D, Filges I, Schmutz NB, Morris MA, Gaide A-C, Dahoun S, Bottani A, Addor M-C, Antonarakis SE, Beckmann JS, Bena F. 2008. Subtelomeric 6p deletion: Clinical and array-CGH characterization in two patients. Am J Med Genet Part A 146A:2094–2102.

Martinez-Glez V, Lorda-Sanchez I, Ramirez JM, Ruiz-Barnes P, Rodriguez de Alba M, Diego-Alvarez D, Ramos C, Searby CC, Nishimura DY, Ayuso C. 2007. Clinical presentation of a variant of Axenfeld–Rieger syndrome associated with subtelomeric 6p deletion. Eur J Med Genet 50:120–127.

Mears AJ, Mirzayans F, Gould DB, Pearce WG, Walter MA. 1996. Autosomal dominant iridogoniodysgenesis anomaly maps to 6p25. Am J Hum Genet 59:1321–1327.

Mears AJ, Jordan T, Mirzayans F, Dubois S, Kume T, Parlee M, Ritch R, Koop B, Kuo WL, Collins C, Marshall J, Gould DB, Pearce W, Carlsson P, Enerbäck S, Morissette J, Bhattacharya S, Hogan B, Raymond V, Walter MA. 1998. Mutations of the forkhead/winged-helix gene, FKHL7, in patients with Axenfeld–Rieger anomaly. Am J Hum Genet 63:1316–1328.

Mirzayans F, Gould DB, Heon E, Billingsley GD, Cheung JC, Mears AJ, Walter MA. 2000. Axenfeld–Rieger syndrome resulting from mutation of the FKHL7 gene on chromosome 6p25. Eur J Hum Genet 8:71–74.

Nishimura DY, Swiderski RE, Alward WL, Searby CC, Patil SR, Bennet SR, Kanis AB, Gastier JM, Stone EM, Sheffield VC. 1998. The forkhead transcription factor gene FKHL7 is responsible for glaucoma phenotypes which map to 6p25. Nat Genet 19:140–147.

Nishimura DY, Searby CC, Alward WL, Walton D, Craig JE, Mackey DA, Kawase K, Kanis AB, Patil SR, Stone EM, Sheffield VC. 2001. A spectrum of FOXC1 mutations suggests gene dosage as a mechanism for developmental defects of the anterior chamber of the eye. Am J Hum Genet 68:364–372.

Perveen R, Lloyd IC, Clayton-Smith J, Churchill A, van Heyningen V, Hanson I, Taylor D, McKeown C, Super M, Kerr B, Winter R, Black GC. 2000. Phenotypic variability and asymmetry of Rieger syndrome

associated with PITX2 mutations. Invest Ophthalmol Vis Sci 41:2456–2460.

Phillips JC, del Bono EA, Haines JL, Pralea AM, Cohen JS, Greff LJ, Wiggs JL. 1996. A second locus for Rieger syndrome maps to chromosome 13q14. Am J Hum Genet 59:613–619.

Priston M, Kozlowski K, Gill D, Letwin K, Buys Y, Levin AV, Walter MA, Héon E. 2001. Functional analyses of two newly identified PITX2 mutants reveal a novel molecular mechanism for Axenfeld–Rieger syndrome. Hum Mol Genet 10:1631–1638.

Saadi I, Semina EV, Amendt BA, Harris DJ, Murphy KP, Murray JC, Russo AF. 2001. Identification of a dominant negative homeodomain mutation in Rieger syndrome. J Biol Chem 276:23034–23041.

Schinzel A, Brecevic L, Dutly F, Baumer A, Binkert F, Largo RH. 1997. Multiple congenital anomalies including the Rieger eye malformation in a boy with interstitial deletion of (4) (q25 → q27) secondary to a balanced insertion in his normal father: Evidence for haplotype insufficiency causing the Rieger malformation. J Med Genet 34:1012–1014.

Semina EV. 2004. PITX2 and PITX3 and the Axenfeld–Rieger syndrome, Iridogoniodysgenesis and iris hypoplasia, Peters anomaly, and anterior segment ocular dysgenesis. In: Epstein CJ, Erickson RP, Wynshaw-Boris A, editors. Oxford monographs on medical genetics no. 49, Molecular basis of developmental malformations. New York: Oxford University Press. pp. 599–606.

Semina EV, Datson NA, Leysens NJ, Zabel BU, Carey JC, Bell GI, Bitoun P, Lindgren C, Stevenson T, Frants RR, van Ommen G, Murray JC. 1996a. Exclusion of epidermal growth factor and high-resolution physical mapping across the Rieger syndrome locus. Am J Hum Genet 59:1288–1296.

Semina EV, Reiter R, Leysens NJ, Alward WL, Small KW, Datson NA, Siegel-Bartelt J, Bierke-Nelson D, Bitoun P, Zabel BU, Carey JC, Murray JC. 1996b. Cloning and characterization of a novel bicoid-related homeobox transcription factor gene, RIEG, involved in Rieger syndrome. Nat Genet 14:392–399.

Shields MB. 1983. Axenfeld–Rieger syndrome: A theory of mechanism and distinctions from the iridocorneal endothelial syndrome. Trans Am Ophthalmol Soc 81:736–784.

Shimokawa O, Miyake N, Yoshimura T, Sosonkina N, Harada N, Mizuguchi T, Kondoh S, Kishino T, Ohta T, Remco V, Takashima T, Kinoshita A, Yoshiura K, Niikawa N, Matsumoto N. 2005. Molecular characterization of del(8)(p23.1p23.1) in a case of congenital diaphragmatic hernia. Am J Med Genet Part A 136A:49–51.

Suzuki T, Takahashi K, Kuwahara S, Wada Y, Abe T, Tamai M. 2001. A novel (Pro79Thr) mutation in the FKHL7 gene in a Japanese family with Axenfeld–Rieger syndrome. Am J Ophthalmol 132:572–575.

Suzuki K, Nakamura M, Amano E, Mokuno K, Shirai S, Terasaki H. 2006. Case of chromosome 6p25 terminal deletion associated with Axenfeld–Rieger syndrome and persistent hyperplastic primary vitreous. Am J Med Genet Part A 140A:503–508.

Swiderski RE, Reiter RS, Nishimura DY, Alward WL, Kalenak JW, Searby CS, Stone EM, Sheffield VC, Lin JJ. 1999. Expression of the Mf1 gene in developing mouse hearts: Implication in the development of human congenital heart defects. Dev Dyn 216:16–27.

SHORT REPORT

Rapid detection of a mutation causing X-linked leucoencephalopathy by exome sequencing

Yoshinori Tsurusaki,[1] Hitoshi Osaka,[2] Haruka Hamanoue,[1] Hiroko Shimbo,[2] Megumi Tsuji,[2] Hiroshi Doi,[1] Hirotomo Saitsu,[1] Naomichi Matsumoto,[1] Noriko Miyake[1]

[1]Department of Human Genetics, Yokohama City University Graduate School of Medicine, Yokohama, Japan
[2]Division of Neurology, Clinical Research Institute, Kanagawa Children's Medical Center, Yokohama, Japan

Correspondence to
Dr Noriko Miyake, Department of Human Genetics, Yokohama City University Graduate School of Medicine, 3-9 Fukuura, Kanazawa-ku, Yokohama 236-0004, Japan;
nmiyake@yokohama-cu.ac.jp

Received 20 October 2010
Revised 14 December 2010
Accepted 5 February 2011
Published Online First
17 March 2011

ABSTRACT

Background Conventional PCR-based direct sequencing of candidate genes for a family with X-linked leucoencephalopathy with unknown aetiology failed to identify any causative mutations.

Objective To carry out exome sequencing of entire transcripts of the whole X chromosome to investigate a family with X linked leucoencephalopathy.

Methods and results Next-generation sequencing of all the transcripts of the X chromosome, after liquid-based genome partitioning, was performed on one of the two affected male subjects (the proband) and an unaffected male subject (his brother). A nonsense mutation in *MCT8* (c.1102A→T (p.R368X)) was identified in the proband. Subsequent PCR-based direct sequencing of other family members confirmed the presence of this mutation, hemizygous in the other affected brother and heterozygous in the proband's mother and maternal grandmother. *MCT8* mutations usually cause abnormal thyroid function in addition to neurological abnormalities, but this proband had normal thyroid function.

Conclusion Single-lane exome next-generation sequencing is sufficient to fully analyse all the transcripts of the X chromosome. This method is particularly suitable for mutation screening of X-linked recessive disorders and can avoid biases in candidate gene choice.

INTRODUCTION

High-throughput, next-generation sequencing (NGS) can have a tremendous impact on human genetic research.[1] Even personal whole-genome analysis is possible,[2] but the cost of obtaining and analysing an entire genome from many people is still unrealistic for many laboratories. Selection and enrichment of regions of interest (genome partitioning) enable us to use NGS efficiently for reasonable numbers of patients with genetic disorders.[3–6]

Ready-to-use microarray-based and solution-based hybridisation systems are now commercially available. A combination of genome partitioning using these systems and NGS is one of the most promising ways to identify genes causing Mendelian disorders.[3 4 6]

Here, we performed exome sequencing of entire transcripts of the whole X chromosome to investigate a family with X linked leucoencephalopathy with unknown aetiology after intensive candidate gene analysis by conventional exon-by-exon Sanger sequencing. A single-lane run of NGS on only two family members successfully determined the leucoencephalopathy-causing mutation.

SUBJECTS AND METHODS

A family with X-linked leucoencephalopathy

The proband (III-2) was a 13-year-old boy. He was born to Japanese consanguineous parents (II-3, 4) after an uneventful pregnancy (figure 1A). His birth weight was 3440 g. Congenital horizontal nystagmus was noted as a neonate. Because of his poor weight gain and developmental delay, he was referred to us at age 5 months. He showed progressive spasticity and dystonia with exaggerated deep tendon reflexes as well as myoclonic and tonic seizures, which responded to valproic acid and clonazepam at age 21 months. Brain MRI at 2 years showed diffuse hyperintensity of the frontal lobe on T2-weighted images, suggesting hypomyelination, and normal T1-weighted images (figure 1B,C). The peak latency intervals in auditory brainstem responses (I–V/III–V) were 4.63/2.37 ms, which were elongated compared with those of age-matched controls (4.24±0.08/1.97±0.08 ms (mean±SD)). He was clinically diagnosed with Pelizaeus–Merzbacher disease (MIM#312080), although neither mutation nor duplication was found in *PLP1* (RefSeq Gene ID, NM_000533) or *GJA12* (NM_020435) (the duplication in *GJA12* was not checked). He was never able to follow objects or control his head.

The dystonia worsened and he is now mechanically ventilated because of tracheomalacia. A thyroid function test at age 13 years indicated all normal levels: free tri-iodothyronine (T_3) 1.2 ng/ml (normal range 0.8–1.6 ng/ml), free thyroxine (T_4) 6.4 μg/dl (normal range 6.1–12.4 μg/dl) and thyroid-stimulating hormone 1.2 μIU/ml (normal range 0.5–5 μIU/ml). Brain MRI at age 13 years demonstrated improvement of myelination in the white matter, but he still presented with severe mental retardation (figure 1D,E). His younger brother was an 8-year-old boy (III-3) with an almost identical clinical course and MRI findings. His grandparents (I-1, I-2) were both healthy. The elder uncle (II-1) died at age 27 years who, initially, could walk with support but who declined towards the end of his life. Another uncle (II-2) was diagnosed with cerebral palsy and died at 7 months of age of unknown causes.

Informed consent was obtained from the patient's family members in accordance with human study protocols approved by the

J Med Genet 2011;**48**:606–609. doi:10.1136/jmg.2010.083535

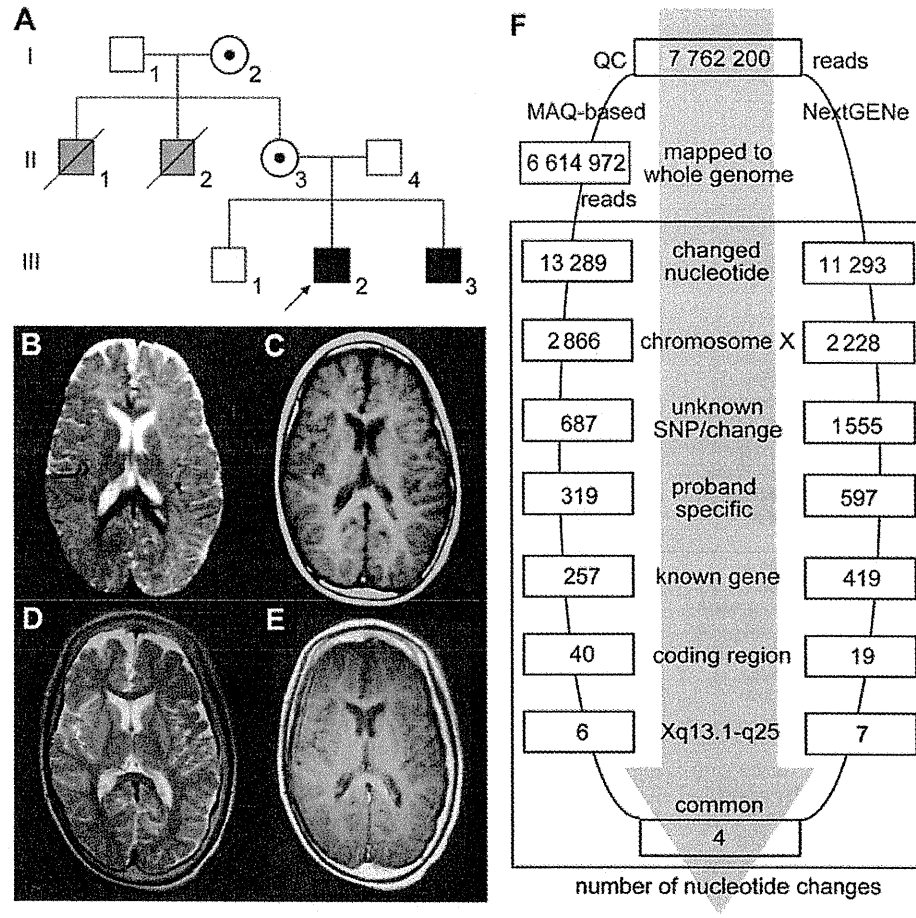

Figure 1 Pedigree and brain MRI of the proband. (A) Family pedigree. (B) T2-weighted image at age 2 years shows diffuse hyperintensity, especially in the frontal lobe. (C) T1-weighted image at 2 years shows nearly complete myelination. (D and E) At age 13 years, both T2 (D) and T1 (E)-weighted images demonstrate complete myelination; the hypomyelination observed at age 2 years can therefore be regarded as delayed myelination. (F) Flow of informatics analysis. A MAQ-based method and NextGENe analysis were performed (III-2). The selection methods included variation relative to the human genome reference sequence; variants mapped to the X chromosome; unknown variants (excluding registered SNPs); variants identified in the proband only (not in his healthy brother); variants in known genes; coding region variants; variants in genes at Xq13.1–q25; and variants common to the two informatics methods. MAQ, Mapping and Assembly with Qualities; SNP, single nucleotide polymorphism.

institutional review board at Kanagawa Children's Medical Centre and Yokohama City University School of Medicine.

Genome-wide single nucleotide polymorphism (SNP) genotyping

Genome-wide SNP genotyping was undertaken for individuals I-1, I-2, II-3, II-4, III-1, III-2 and III-3 using the GeneChip Human Mapping 10K Array *Xba* 142 2.0 (Affymetrix Inc, Santa Clara, California, USA), according to the manufacturer's protocols. Mendelian errors in the pedigree to exclude conflicted SNPs were checked using GeneChip operating software 1.2 (Affymetrix) and batch analysis in GeneChip genotyping analysis software 4.0 (Affymetrix), with the default settings for a mapping algorithm. Copy Number Analyzer for GeneChip 2.0 was used to validate copy number alterations.[7] The linked region with SNPs shared between individuals III-2 and III-3 (not observed in III-1) was checked manually.

Genome partitioning, short-read sequencing and sequence alignment

Genomic DNAs from the proband (III-2) and his unaffected brother (III-1) were used for this study. Three micrograms of DNA were processed using a SureSelect X chromosome test kit (1582 transcripts covering 3053 kb) (Agilent Technologies, Santa Clara, California, USA), according to the manufacturer's instructions. Captured DNAs were analysed using an Illumina GAIIx (Illumina Inc, San Diego, California, USA). We used only one of the eight lanes of the flow cell (Illumina), performing single 76 bp reads for each sample. Image analysis and base calling were performed by sequence control software (SCS) real-time analysis (Illumina) and/or offline Basecaller software v1.6 (Illumina) and CASAVA software v1.6 (Illumina). Reads were aligned to the human reference genome sequence (UCSC hg18, NCBI build 36.1) using the ELAND v2 program (Illumina). Coverage was calculated statistically. Identified variants were annotated based on novelty, impact on the encoded protein, the number and frequency of reads and conservation. NextGENe software v1.99 (SoftGenetics, State College, Pennsylvania, USA) was also used to analyse reads, with the default settings.

Mapping strategy and variant annotation

Approximately 9.9 million reads from III-1 (the unaffected sibling) and 7.8 million reads from III-2 (the proband), which passed the quality control (Path Filter), were mapped to the human reference genome by Mapping and Assembly with Qualities (MAQ)[8] and NextGENe software (SoftGenetics) (figure 1F). The bait region of the X chromosome based on the manufacturer's information was carefully evaluated. MAQ was able to align 7 359 688 and 6 614 972 reads to the whole genome for III-1 and III-2, respectively, which were statistically analysed for coverage using a script created by BITS Co Ltd (Tokyo, Japan). SNPs and indels were extracted from the alignment data using another script created by BITS, along with information on registered SNPs (dbSNP build 130). A consensus quality score of ≥40 was used for the SNP analysis in MAQ.

Capillary sequencing

Possible pathological variants were confirmed by Sanger sequencing using an ABI 3500xl or ABI3100 autosequencer (Life Technologies, Carlsbad, California, USA), following the manufacturer's protocol. Sequencing data were analysed by

Sequencher software (Gene Codes Corporation, Ann Arbor, Michigan, USA).

RESULTS AND DISCUSSION

Coverage analysis showed that 78.9% of all the X chromosome transcripts were completely covered by reads, and that 11.6% of transcripts were at least 90% covered. Almost all (99%) of these regions were covered by 20 reads or more (100 reads or more in 97%) by only single-lane sequencing. SNP genotyping was able to delineate the minimal linked region from rs763739 to rs1073455 (UCSC genome browser hg19 assembly, X chromosome coordinates: 76 804 990–126 844 262) (50 Mb). The maximum linked region was from rs1926354 to rs859587 (UCSC genome browser coordinates: 68 404 915–128 933 907) (60.5 Mb). Exome GAIIx sequencing with the two informatics methods identified four potentially interesting changes in the maximum linked region: c.1102AT (p.R368X) in *MCT8* (NM_006517; alternatively called *SLC16A2*); c.1402T→G (p.S468A) and c.1943A→G (p.H648R) in *CYLC1* (NM_021118); and c1606G→A (p.D536N) in *LRCH2* (NM_020871) (figure 1F). c.1102A→T (p.R368X) in *MCT8* was found heterozygously in the proband's healthy mother (II-3) and maternal grandmother (I-2), and hemizygously in the proband and his affected younger brother; each was confirmed by Sanger sequencing (figure 2). This change was not present among 92 normal female controls (0/184 alleles).

The *MCT8* gene encodes a thyroid hormone transporter and is implicated in syndromic X-linked mental retardation, Allan–Herndon–Dudley syndrome and Pelizaeus–Merzbacher-like disease (PMLD).[9–12] This nonsense mutation, c.1102A→T (p.R368X), which might lead to nonsense-mediated decay resulting in no protein production, is highly likely to be pathological. Based on the human gene mutation database (http://www.hgmd.cf.ac.uk/ac/index.php), three nonsense mutations in this gene have been previously registered: p.R245X, p.Q335X and p.S448X. The other identified variants, in *CYLC1* and *LRCH2*, are all SNPs because they were identified in normal controls: c.1402T→G (*CYLC1*): 5/182 alleles, c.1943A→G (*CYLC1*): 12/184 alleles and c1606G→A (*LRCH2*): 5/184 alleles. We concluded that the *MCT8* mutation was pathogenic in this family.

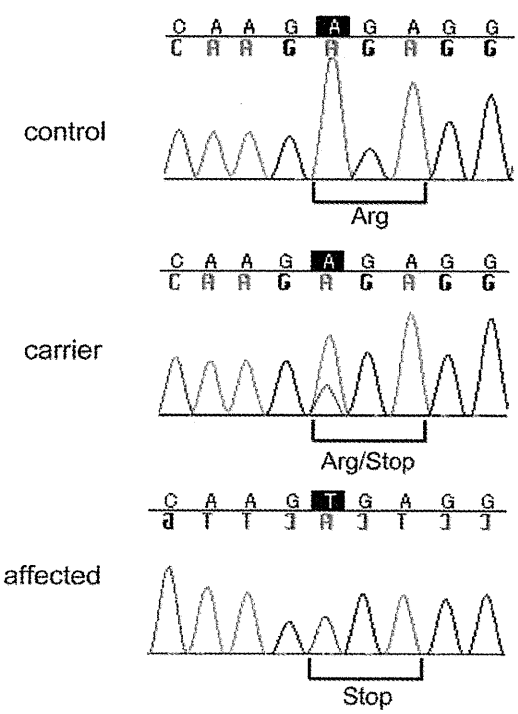

Figure 2 Electropherograms of a normal control, a carrier (mother) and the affected proband.

PMLD caused by *MCT8* mutations presents with infantile hypotonia, severe psychomotor development, nystagmus, generalised muscle weakness, dystopia, joint contracture and progressive spastic paraplegia. All affected male subjects develop the disease, while heterozygous female subjects are clinically normal or sometimes show mild thyroid dysfunction.[9 12] Brain MRI shows delayed myelination in the first few years of life, which subsequently improves but with residual neurological disability. The unique diagnostic feature of the disease is an abnormal thyroid hormone profile: increased free T_3, decreased free T_4 and normal thyroid-stimulating hormone.[12] The cases we analysed here showed clinical features and brain MRI findings typical of PMLD, but no thyroid hormone abnormalities. Based on regular laboratory testing and conventional PCR-based gene screening, we might have failed, or taken much longer, to identify the causative mutation. Thus, unbiased screening without prior knowledge is one of the advantages of NGS.

Thyroid hormone (T_4 and T_3) is important in neuronal development and its deficiency in the pre/neonatal stage causes a form of mental retardation called cretinism. T_4 is released from the thyroid as a prohormone and is altered to biologically active T_3 by iodothyronine deiodinases.[13] Active T_3 is delivered to the peripheral organs via thyroid hormone transporters. MCT8 is a thyroid hormone-specific transporter and is mainly expressed in the brain and liver.[14 15] In MCT8 deficiency, T_3 and T_4 uptake is impaired and deiodinase 2 is activated.[16] This results in increased serum T_3 levels because of T_3 accumulation in the peripheral blood. In previous reports, the majority of patients showed abnormal levels of thyroid hormones, but some displayed values within the normal range.[9 10 12 17 18] The variable range for abnormal thyroid hormone levels might be explained by unidentified modifier effect(s) and/or other transporter(s) that can compensate for MCT8 function.[19] Additionally, although MCT8 deficiency has been determined by abnormalities in thyroid function tests, it is unknown what proportion of the patients with MCT8 deficiency show abnormal thyroid function. We suggest that it is important to evaluate thyroid hormone function in PMLD with unknown cause.

Before the exome NGS analysis, we screened *PLP1*, *GJA12*, and seven other candidate genes mapped to the linked region: *MSN* (NM_002444), *IGBP1* (NM_001551), *SNX12* (NM_013346), *OGT* (NM_181672), *HDAC8* (NM_018486), *SH3BGRL* (NM_003022.2) and *PCDH11X* (NM_032967.2). Because we found no pathological changes, we adopted the exome sequencing strategy. We determined that exome sequencing with a single lane for each sample was sufficient to analyse all the transcripts of the X chromosome. In X-linked recessive diseases, male subjects are usually affected, and therefore the single X chromosome is the primary target of exome sequencing. Except for mosaic mutations, the hemizygous (rather than heterozygous) status of disease-related nucleotide changes is relatively easy to detect using all-or-none NGS reads (0% or 100% of reads). There was no difference in the ability of our two informatics methods (MAQ and NextGENe) to detect pathological changes. This approach could equally be applied to the analysis

of autosomal recessive diseases that manifest in the offspring of consanguineous relationships.

In conclusion, we rapidly identified a nonsense mutation in *MCT8* in a family with X-linked leucoencephalopathy using only a single lane of exome sequencing. This method is powerful for unbiased screening of disease-related mutations in X-linked or recessive conditions.

Acknowledgements We thank the family for their participation in this study.

Funding This work was supported by research grants from the Ministry of Health, Labour and Welfare (to HO, HSa, NMa and NMi), a grant-in-aid for scientific research from the Japan Society for the Promotion of Science (NMa), a grant-in-aid for young scientists from the Japan Society for the Promotion of Science (HSa), a grant from the 2010 Strategic Research Promotion of Yokohama City University (NMa), research grants from the Japan Epilepsy Research Foundation (HSa) and a research grant from the Naito Foundation (NMa). The study sponsors had no role in the study design; in the collection, analysis, and interpretation of the data; in the writing of the report; or in the decision to submit the paper for publication.

Competing interests None.

Patient consent Obtained.

Ethics approval This study was conducted with the approval of the institutional review board of Kanagawa Children's Medical Center and Yokohama City University School of Medicine.

Provenance and peer review Not commissioned; externally peer reviewed.

REFERENCES

1. **Shendure J,** Ji H. Next-generation DNA sequencing. *Nat Biotechnol* 2008;**26**:1135–45.
2. **Wheeler DA,** Srinivasan M, Egholm M, Shen Y, Chen L, McGuire A, He W, Chen YJ, Makhijani V, Roth GT, Gomes X, Tartaro K, Niazi F, Turcotte CL, Irzyk GP, Lupski JR, Chinault C, Song XZ, Liu Y, Yuan Y, Nazareth L, Qin X, Muzny DM, Margulies M, Weinstock GM, Gibbs RA, Rothberg JM. The complete genome of an individual by massively parallel DNA sequencing. *Nature* 2008;**452**:872–6.
3. **Ng SB,** Turner EH, Robertson PD, Flygare SD, Bigham AW, Lee C, Shaffer T, Wong M, Bhattacharjee A, Eichler EE, Bamshad M, Nickerson DA, Shendure J. Targeted capture and massively parallel sequencing of 12 human exomes. *Nature* 2009;**461**:272–6.
4. **Choi M,** Scholl UI, Ji W, Liu T, Tikhonova IR, Zumbo P, Nayir A, Bakkaloglu A, Ozen S, Sanjad S, Nelson-Williams C, Farhi A, Mane S, Lifton RP. Genetic diagnosis by whole exome capture and massively parallel DNA sequencing. *Proc Natl Acad Sci U S A* 2009;**106**:19096–101.
5. **Hodges E,** Xuan Z, Balija V, Kramer M, Molla MN, Smith SW, Middle CM, Rodesch MJ, Albert TJ, Hannon GJ, McCombie WR. Genome-wide in situ exon capture for selective resequencing. *Nat Genet* 2007;**39**:1522–7.
6. **Ng SB,** Buckingham KJ, Lee C, Bigham AW, Tabor HK, Dent KM, Huff CD, Shannon PT, Jabs EW, Nickerson DA, Shendure J, Bamshad MJ. Exome sequencing identifies the cause of a mendelian disorder. *Nat Genet* 2010;**42**:30–5.
7. **Nannya Y,** Sanada M, Nakazaki K, Hosoya N, Wang L, Hangaishi A, Kurokawa M, Chiba S, Bailey DK, Kennedy GC, Ogawa S. A robust algorithm for copy number detection using high-density oligonucleotide single nucleotide polymorphism genotyping arrays. *Cancer Res* 2005;**65**:6071–9.
8. **Li H,** Ruan J, Durbin R. Mapping short DNA sequencing reads and calling variants using mapping quality scores. *Genome Res* 2008;**18**:1851–8.
9. **Dumitrescu AM,** Liao XH, Best TB, Brockmann K, Refetoff S. A novel syndrome combining thyroid and neurological abnormalities is associated with mutations in a monocarboxylate transporter gene. *Am J Hum Genet* 2004;**74**:168–75.
10. **Friesema EC,** Grueters A, Biebermann H, Krude H, von Moers A, Reeser M, Barrett TG, Mancilla EE, Svensson J, Kester MH, Kuiper GG, Balkassmi S, Uitterlinden AG, Koehrle J, Rodien P, Halestrap AP, Visser TJ. Association between mutations in a thyroid hormone transporter and severe X-linked psychomotor retardation. *Lancet* 2004;**364**:1435–7.
11. **Frints SG,** Lenzner S, Bauters M, Jensen LR, Van Esch H, des Portes V, Moog U, Macville MV, van Roozendaal K, Schrander-Stumpel CT, Tzschach A, Marynen P, Fryns JP, Hamel B, van Bokhoven H, Chelly J, Beldjord C, Turner G, Gecz J, Moraine C, Raynaud M, Ropers HH, Froyen G, Kuss AW. *MCT8* mutation analysis and identification of the first female with Allan-Herndon-Dudley syndrome due to loss of *MCT8* expression. *Eur J Hum Genet* 2008;**16**:1029–37.
12. **Vaurs-Barriere C,** Deville M, Sarret C, Giraud G, Des Portes V, Prats-Vinas JM, De Michele G, Dan B, Brady AF, Boespflug-Tanguy O, Touraine R. Pelizaeus-Merzbacher-Like disease presentation of *MCT8* mutated male subjects. *Ann Neurol* 2009;**65**:114–18.
13. **Bianco AC,** Salvatore D, Gereben B, Berry MJ, Larsen PR. Biochemistry, cellular and molecular biology, and physiological roles of the iodothyronine selenodeiodinases. *Endocr Rev* 2002;**23**:38–89.
14. **Friesema EC,** Ganguly S, Abdalla A, Manning Fox J, Halestrap AP, Visser TJ. Identification of monocarboxylate transporter 8 as a specific thyroid hormone transporter. *J Biol Chem* 2003;**41**:40128–35.
15. **Lafreniere RG,** Carrel L, Willard HF. A novel transmembrane transporter encoded by the XPCT gene in Xq13.2. *Hum Mol Genet* 1994;**3**:1133–9.
16. **Dumitrescu AM,** Liao XH, Weiss RE, Millen K, Refetoff S. Tissue-specific thyroid hormone deprivation and excess in monocarboxylate transporter (mct) 8-deficient mice. *Endocrinology* 2006;**147**:4036–43.
17. **Maranduba CM,** Friesema EC, Kok F, Kester MH, Jansen J, Sertie AL, Passos-Bueno MR, Visser TJ. Decreased cellular uptake and metabolism in Allan-Herndon-Dudley syndrome (AHDS) due to a novel mutation in the MCT8 thyroid hormone transporter. *J Med Genet* 2006;**43**:457–60.
18. **Namba N,** Etani Y, Kitaoka T, Nakamoto Y, Nakacho M, Bessho K, Miyoshi Y, Mushiake S, Mohri I, Arai H, Taniike M, Ozono K. Clinical phenotype and endocrinological investigations in a patient with a mutation in the MCT8 thyroid hormone transporter. *Eur J Pediatr* 2008;**167**:785–91.
19. **Herzovich V,** Vaiani E, Marino R, Dratler G, Lazzati JM, Tilitzky S, Ramirez P, Iorcansky S, Rivarola MA, Belgorosky A. Unexpected peripheral markers of thyroid function in a patient with a novel mutation of the MCT8 thyroid hormone transporter gene. *Horm Res* 2007;**67**:1–6.

De novo mutations in epilepsy

Ohtahara syndrome and West syndrome are considered to be a continuum of early-onset epileptic encephalopathies, because the majority (75%) of Ohtahara syndrome cases evolve into West syndrome. Brain malformations are frequently associated with Ohtahara syndrome and West syndrome. The presence of cryptogenic cases suggests genetic factors may also be involved. However, most cases of these syndromes are sporadic, probably because of their poor clinical outcomes with severe psychomotor impairment.

De novo copy number variations (CNVs) and mutations are major causes of sporadic traits.[1] Their occurrence has been estimated to be 1.7×10^{-6} per locus and $2.2–4.0 \times 10^{-8}$ per nucleotide in a diploid embryo respectively, suggesting that an average newborn is expected to acquire approximately 0.86 amino acid altering mutations, and that de novo CNVs are more frequent than de novo mutations.[1–3] Increased availability of genomic microarrays, such as array comparative genomic hybridization, has facilitated the detection of de novo CNVs in which disease-causative genes may reside.

We have recently identified two disease-causative genes (*STXBP1* for Ohtahara syndrome and *SPTAN1* for a type of West syndrome) through identification of a de novo microdeletion at 9q33.3-q34.11 in one of four individuals (participant 1) with early-onset West syndrome with severe cerebral hypomyelination.[4–6] Among more than 40 genes within the deletion, we focused firstly on *STXBP1*, because it is involved in synaptic vesicle release and has brain-specific expression in both rodents and humans. Participant 1 was initially diagnosed with Ohtahara syndrome, which progressed to West syndrome at 3 months of age. *STXBP1* screening in other patients with Ohtahara syndrome with no brain anomalies led to the identification of four missense mutations, indicating that mutations in *STXBP1* cause cryptogenic Ohtahara syndrome.[4] To date, *STXBP1* abnormalities have been found in 19 out of 55 individuals (34.5%) with cryptogenic Ohtahara syndrome (including unpublished data).[7] Seventeen out of 19 deletions or mutations were confirmed as de novo events. The remaining two included an inherited mutation from the somatic-mosaic father, and an unconfirmed mutation due to unavailability of paternal DNA. Moreover, the clinical spectrum of *STXBP1* mutations has been shown to be broader. Aberrations of *STXBP1* were found in six out of 106 patients with early-onset epileptic encephalopathies (five mutations/deletions occured de novo).[8] Of note, the initial phenotype of five patients with *STXBP1* aberrations did not fit into either Ohtahara syndrome or West syndrome.[8] Furthermore, two de novo *STXBP1* mutations were also found in two out of 95 individuals with learning disability* and non-syndromic epilepsy.[9] These findings indicated that CNV and mutation screening in *STXBP1* should be considered in children with early-onset seizures.

Were there *STXBP1* mutations in the remaining three participants with early-onset West syndrome with severe cerebral hypomyelination? We could not find any *STXBP1* abnormalities in two of the remaining three participants (one was unavailable). While most patients with *STXBP1* mutations showed normal myelination, participant 1 additionally showed severe hypomyelination of the cerebral cortex and a thin corpus callosum at 12 months of age.[5] Therefore we hypothesized that another gene within the deletion may contribute to severe hypomyelination in participant 1. The *SPTAN1* gene encoding α-II spectrin appeared to be a primary candidate because zebrafish α-II spectrin mutants showed impaired myelination, and de novo in-frame mutations in *SPTAN1* were identified in the remaining two participants, suggesting that mutations in *SPTAN1* cause early-onset West syndrome with severe hypomyelination. Our identification of two disease genes from one de novo deletion in a single case may be a rare event; however, it should be emphasized that careful evaluation of clinical and molecular data in detail may reveal occult, yet important, findings.

In addition to *STXBP1* and *SPTAN1*, de novo mutations in *SCN1A*, *CDKL5*, and *ARX* genes have been reported in early-onset epileptic encephalopathies. Thus, it is likely that de novo mutations of known and unknown causative genes are a common cause of early-onset epileptic encephalopathies, which mostly occur sporadically. Recent progress in massively parallel DNA sequencing enables us to rapidly detect point mutations, and de novo mutations could be systemically identified by family-based exome sequencing (using trios: one patient and parents).[10] Together with genomic microarray, exome sequencing is likely to be provided as a clinical service in the near future, and will undoubtedly demonstrate important roles of de novo CNVs and mutations in early-onset epileptic encephalopathies.

HIROTOMO SAITSU
NAOMICHI MATSUMOTO
Department of Human Genetics, Graduate School of Medicine, Yokohama City University, Yokohama, Japan.

doi: 10.1111/j.1469-8749.2011.03994.x

*North American usage: mental retardation.

REFERENCES

1. Lupski JR. Genomic rearrangements and sporadic disease. *Nat Genet* 2007; **39:** S43–7.
2. Lynch M. Rate, molecular spectrum, and consequences of human mutation. *Proc Natl Acad Sci USA* 2010; **107:** 961–8.
3. Roach JC, Glusman G, Smit AF, et al. Analysis of genetic inheritance in a family quartet by whole-genome sequencing. *Science* 2010; **328:** 636–9.
4. Saitsu H, Kato M, Mizuguchi T, et al. De novo mutations in the gene encoding STXBP1 (MUNC18-1) cause early infantile epileptic encephalopathy. *Nat Genet* 2008; **40:** 782–8.
5. Tohyama J, Akasaka N, Osaka H, et al. Early onset West syndrome with cerebral hypomyelination and reduced cerebral white matter. *Brain Dev* 2008; **30:** 349–55.
6. Saitsu H, Tohyama J, Kumada T, et al. Dominant-negative mutations in alpha-II spectrin cause West syndrome with severe cerebral hypomyelination, spastic quadriplegia, and developmental delay. *Am J Hum Genet* 2010; **86:** 881–91.
7. Saitsu H, Kato M, Okada I, et al. *STXBP1* mutations in early infantile epileptic encephalopathy with suppression-burst pattern. *Epilepsia* 2010; **51:** 2397–405.
8. Deprez L, Weckhuysen S, Holmgren P, et al. Clinical spectrum of early-onset epileptic encephalopathies associated with STXBP1 mutations. *Neurology* 2010; **75:** 1159–65.
9. Hamdan FF, Piton A, Gauthier J, et al. De novo STXBP1 mutations in mental retardation and nonsyndromic epilepsy. *Ann Neurol* 2009; **65:** 748–53.
10. Vissers LE, de Ligt J, Gilissen C, et al. A de novo paradigm for mental retardation. *Nat Genet* 2010; **42:** 1109–12.

CLINICAL GENETICS An International Journal of Genetics, Molecular and Personalized Medicine

Clin Genet 2011: 80: 161–166
Printed in Singapore. All rights reserved

CLINICAL GENETICS
doi: 10.1111/j.1399-0004.2011.01721.x

Short Report

Exome sequencing of two patients in a family with atypical X-linked leukodystrophy

Tsurusaki Y, Okamoto N, Suzuki Y, Doi H, Saitsu H, Miyake N, Matsumoto N. Exome sequencing of two patients in a family with atypical X-linked leukodystrophy.
Clin Genet 2011: 80: 161–166. © John Wiley & Sons A/S, 2011

We encountered a family with two boys similarly showing brain atrophy with reduced white matter, hypoplasia of the brain stem and corpus callosum, spastic paralysis, and severe growth and mental retardation without speaking a word. The phenotype of these patients was not compatible with any known type of syndromic leukodystrophy. Presuming an X-linked disorder, we performed next-generation sequencing (NGS) of the transcripts of the entire X chromosome. A single lane of exome NGS in each patient was sufficient. Six potential mutations were found in both affected boys. Two missense mutations, including c.92T>C (p.V31A) in *L1CAM*, were potentially pathogenic, but this remained inconclusive. The other four could be excluded. Because the patients did not show adducted thumbs or hydrocephalus, the *L1CAM* change in this family can be interpreted as different scenarios. Personal genome analysis using NGS is certainly powerful, but interpretation of the data can be a substantial challenge requiring a lot of tasks.

Conflict of interest

None of the authors have any conflicts of interest to disclose.

Y Tsurusaki[a], N Okamoto[b], Y Suzuki[c], H Doi[a], H Saitsu[a], N Miyake[a] and N Matsumoto[a]

[a]Department of Human Genetics, Yokohama City University Graduate School of Medicine, Kanazawa-ku, Yokohama, Japan, and [b]Department of Medical Genetics, and [c]Department of Pediatric Neurology, Osaka Medical Center and Research Institute for Maternal and Child Health, Murodo-cho, Izumi, Japan

Key words: atypical phenotype – exome sequencing – *L1CAM* – X-linked leukodystrophy

Corresponding author: Naomichi Matsumoto, Department of Human Genetics, Yokohama City University Graduate School of Medicine, 3-9 Fukuura, Kanazawa-ku, Yokohama 236-0004, Japan.
Tel.: +81-45-787-2606;
fax: +81-45-786-5219;
e-mail: naomat@yokohama-cu.ac.jp

Received 4 May 2011, revised and accepted for publication 31 May 2011

Focused/selected gene and genomic characterization has usually been carried out in clinically homogeneous groups of multiple affected samples to make identification of genetic abnormalities more efficient. Microarrays and next-generation sequencing (NGS) have provided new avenues for human genetic research (1–6). Using such new technologies, researchers are able to analyze small numbers of patients on a genome-wide scale. Even very rare cases (such as when only a few compatible patients are available or atypical patients showing no similar phenotypes) can be realistic targets of genetic research, as the new technologies can identify aberrations in a single gene from within virtually the whole genome; this could not be achieved with conventional techniques.

We encountered a family with two affected males showing atypical leukodystrophy. The phenotype of these patients did not match any known type of syndromic leukodystrophy. Because we presumed that abnormality of an X-linked gene caused the atypical leukodystrophy in this family, we performed exome sequencing of most of the X-chromosome transcripts and identified an unexpected gene mutation in these patients.

Materials and methods

A family with atypical X-linked leukodystrophy

Two brothers, II-1 currently aged 19 years and II-2 currently aged 17 years, who have unrelated healthy parents, presented with similar clinical

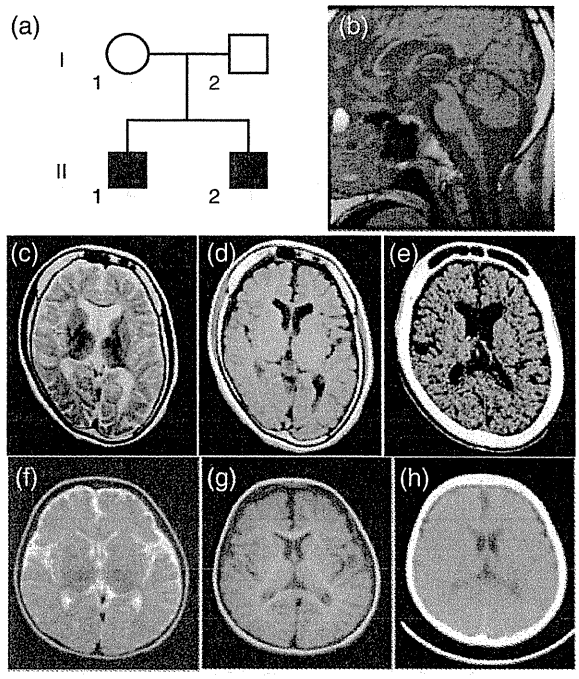

Fig. 1. Clinical features of the family. Familial pedigree (**a**). Brain magnetic resonance imaging (MRI) (**b**: T1-weighted image, **c**: T2-weighted image, **d**: T1-weighted image) of individual II-1 at 16 years old showing hypoplasia of the white matter, the brain stem and the corpus callosum. Brain computed tomographic (CT) images of individual II-1 at 19 years old (**e**) indicating a thick calvarium with enlarged frontal sinus as well as calcification of the choroid plexus in the atrophic brain. Brain MRI (**f**: T2-weighted image, **g**: T1-weighted image) of individual II-2 at 2 years old, also displaying hypoplasia of the white matter. Brain CT image of individual II-2 at 5 years old (**h**), also showing a thick calvarium.

features. Their mother did not show any neurological abnormalities (Fig. 1a).

Patient II-1

Patient II-1's birth weight was 2840 g at 40 weeks of gestational age. He had congenital nystagmus. He sat unsupported at 7 months old but after this his developmental milestones were delayed. He could creep at 18 months old. Spastic paralysis, especially in the lower extremities, became apparent. He was unable to stand unsupported. His mental development was severely delayed, and he needed special education from elementary school. He had suffered generalized epileptic seizures since he was 10 years old. He was confined to a wheelchair. He had severe mental retardation without speaking a word. His developmental quotient (DQ) at 9 years old was 19 by the Japanese standard method. Severe growth retardation [143 cm (<3%), 24 kg (<3%), occipitofrontal head circumference 49 cm (<3%) at 19 years] was also noted. He did not have dysmorphic features. Blood analysis revealed microcytic anemia [hemoglobin (Hb) 13.4 g/dl, mean corpuscular volume (MCV) (of red blood cell) 70.4 fl (normal: 89–99 fl), mean corpuscular hemoglobin (MCH) (of red blood cell) 23.1 pg (normal: 29–35 pg)] without any evidence of hemolysis or iron deficiency. Hormonal examination indicated that the levels of luteinizing hormone, follicle-stimulating hormone, and thyroid-stimulating hormone were all low [0.9 mIU/ml (normal: 1.2–8.0 mIU/ml), 2.5 mIU/ml (normal: 2.3–15.1 mIU/ml), <0.01 μIU/ml (normal: 0.5–5.0 μIU/ml), respectively]. He showed delayed puberty with small testes. Pubic hair only appeared at 17 years old. His bone age at 18 years old was 12.6 years (67%). Brain magnetic resonance imaging (MRI) at 16 years old revealed brain atrophy associated with reduced white matter and hypoplasia of the brain stem and the corpus callosum (Fig. 1b–d). No hydrocephalus or adducted thumb was observed. Brain computed tomography (CT) at 19 years old showed a thick calvarium with enlarged frontal sinus as well as calcification of the cerebellar tentorium and the choroid plexus (Fig. 1e).

Patient II-2

Patient II-2's birth weight was 2910 g at 37 weeks of gestational age. Developmental delay was apparent since he was 10 months old. Spastic paralysis (especially in the lower extremities), confinement to a wheelchair, severe mental retardation without speaking a word (DQ = 5 at 17 years old), and severe growth retardation [130 cm (<3%) and 27 kg (<3%) at 17 years] were phenotypes shared with his brother (II-1). Blood analysis revealed microcytic anemia (Hb 12.0 g/dl, MCV 61.1 fl, MCH 19.0 pg) without any evidence of hemolysis or iron deficiency. Hormonal examination indicated that the levels of luteinizing hormone, follicle-stimulating hormone, and thyroid-stimulating hormone were relatively low (1.9 mIU/ml, 4.2 mIU/ml, <0.23 μIU/ml, respectively). He also showed delayed puberty with small testes. Pubic hair appeared only at 17 years old. His bone age at 17 years old was 11 years (65%). Brain MRI at 2 years old revealed brain atrophy associated with reduced white matter and hypoplasia of the brain stem and corpus callosum (Fig. 1f,g). Brain CT at 5 years old showed a thick calvarium (Fig. 1h). No hydrocephalus or adducted thumb was observed. Most of the clinical features were similar to those of his brother except for the absence of nystagmus in patient II-2.

Genome-wide SNP genotyping

Genome-wide single-nucleotide polymorphism (SNP) genotyping was performed on individuals I-2, II-1, and II-2 using a GeneChip™ Human Mapping 10K Array Xba 142 2.0 (Affymetrix, Inc., Santa Clara, CA), according to the manufacturer's protocols. Mendelian error in the pedigree to exclude conflicted SNPs was checked using GCOS 1.2 (GeneChip Operating Software; Affymetrix) and batch analysis in GTYPE 4.0 (GeneChip Genotyping Analysis Software; Affymetrix), with the default setting for the mapping algorithm. The linked region, with SNP genotypes shared between individuals II-1 and II-2, was checked manually.

Genomic partitioning, short-read sequencing, and sequence alignment

Three micrograms of genomic DNA from the affected brothers (II-1 and II-2) was processed using a SureSelect X Chromosome test kit (1582 transcripts covering 3053 kb) (Agilent Technologies, Santa Clara, CA), according to the manufacturer's instructions. Captured DNAs were analyzed using an Illumina GAIIx (Illumina, Inc., San Diego, CA). We used only one of the eight lanes in the flow cell (Illumina) for paired-end, 76-bp reads per sample. Image analysis and base-calling were performed using sequence control software (SCS) real-time analysis and off-line BASECALLER software v1.8.0 (Illumina). Reads were aligned to the human reference genome (UCSC hg19, NCBI build 37.1) using the ELANDv2 algorithm in CASAVA_v1.7.0 (Illumina). The ELANDv2 algorithm can align 100-bp reads to a reference sequence and split the reads into multiple seeds.

Mapping strategy and variant annotation

Approximately 57.5 million reads from individual II-1 and 71.1 million reads from individual II-2 that passed the quality control (Path Filter) were mapped to the human reference genome using mapping and assembly with quality (MAQ) (7) (Fig. 2). MAQ was able to align 51 720 952 and 65 990 660 reads to the whole genome for individuals II-1 and II-2, respectively; these were then statistically analyzed for coverage using a script created by BITS Co., Ltd. (Tokyo, Japan). SNPs and insertions/deletions were extracted from the alignment data using an original script created by BITS Co., Ltd., along with information on the registered SNPs (dbSNP 131). A consensus quality score of 40 or more was used for the SNP analysis in MAQ. SNPs in MAQ-passed reads were annotated using the SeattleSeq website (http://gvs.gs.washington.edu/SeattleSeqAnnotation/). Variants found by each informatics method were selected in terms of location on chromosome X, unregistered variants (excluding registered SNPs), variants in known genes, variants in coding regions, variants excluding synonymous changes, and variants with an allele frequency of at least 90% (assuming a homozygous mutation). NEXTGENE software v2.0 (SoftGenetics, State College, PA) was also used to analyze the reads, with a default setting. Variants found by both of the informatics methods were selected. The variants found in common between individuals II-1 and II-2 were focused on, and confirmed as true positives by Sanger sequencing of polymerase chain reaction (PCR) products amplified from patient genomic DNA, except for variants within genes at segmental duplications. The pathological significance of the variants was evaluated using four different websites: POLYPHEN (Polymorphism Phenotyping; http://genetics.bwh.harvard.edu/pph/index.html), POLYPHEN-2 (http://genetics.bwh.harvard.edu/pph2/index.shtml), SIFT (http://sift.jcvi.org/) (output values less than 0.05 are deleterious), and MUTATIONTASTER (http://neurocore.charite.de/MutationTaster/).

Capillary sequencing

Possible pathological variants were confirmed by Sanger sequencing using an ABI 3500xl or ABI3100 autosequencer (Life Technologies, Carlsbad, CA), following the manufacturer's protocol. Sequencing data were analyzed using SEQUENCHER software (Gene Codes Corporation, Ann Arbor, MI).

Expression studies

The relative mRNA levels of *TMEM187* in cDNA of various fetal and adult human tissues (Human MTC™ Panel I and Human Fetal MTC™ Panel; Clontech, Mountain View, CA) were determined by quantitative real-time reverse transcription–polymerase chain reaction (RT-PCR) using TaqMan gene expression assays (Hs01920894_s1 for *TMEM187* and Hs00357333_g1 for β-actin as a control) (Life Technologies).

Results and discussion

Our coverage analysis indicated that for individuals II-1 and II-2, 79.2% and 78.8%, respectively, of the entire X-chromosome coding sequence (CDS) were completely covered, and 88.5% and 88.5%,

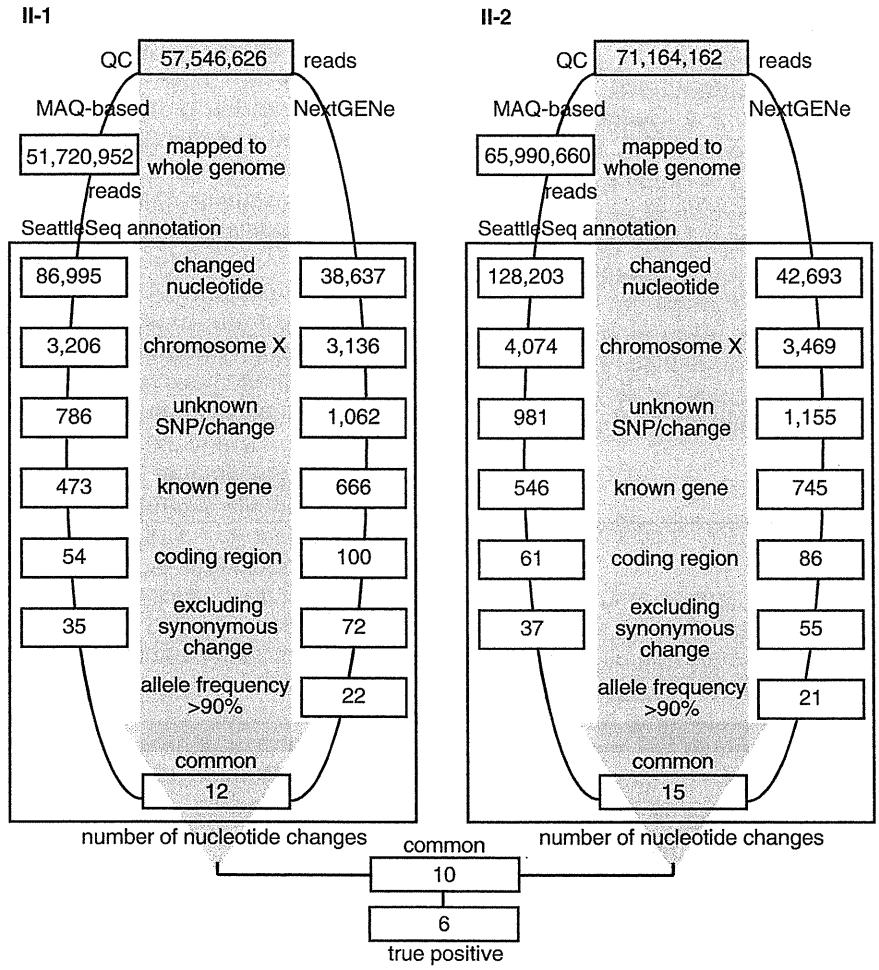

Fig. 2. Flow of informatics analysis. A MAQ-based method and NextGENe analysis were performed in individuals II-1 and II-2. The selection methods employed included variants compared with the human genome reference sequence, variants mapped to chromosome X, unknown variants [excluding registered single-nucleotide polymorphisms (SNPs)], variants in known genes, variants in coding regions, variants excluding synonymous changes, and variants common to the two informatics methods. Finally, the nucleotide changes in common between individuals II-1 and II-2 were focused on as potentially pathogenic mutations. True positive changes were confirmed by capillary sequencing of polymerase chain reaction (PCR) products amplified from genomic DNA.

respectively, of the CDS were at least 90% covered by reads. Using a single lane of sequencing per sample, the coverage with 20 reads or more comprised 89.6% and 89.7% of the CDS, and that with 100 reads or more comprised 87.6% and 89.7% of the CDS in individuals II-1 and II-2, respectively. SNP genotyping indicated that the region from rs727240 to rs721003 (UCSC genome browser hg19 assembly, chromosome X coordinates: 22131639–54454152; 32.2 Mb) was unlinked to the phenotype. Exome sequencing using two informatics methods successfully identified six potentially interesting changes as true positives in the linked region: *FAM123B* (RefSeq Gene ID NM_152424): c.85G>A (p.A29T), *FRMD7* (NM_194277): c.875T>C (p.L292P), *L1CAM* (NM_000425): c.92T>C (p.V31A), *TMEM187* (NM_003492): c.334G>A (p.A112T), *FLNA* (NM_001110556): c.1582G>A (p.V528M), and *LAGE3* (NM_006014): c.395G>A (p.R132Q).

The c.92T>C (p.V31A) variant in *L1CAM* was previously found in a patient with Hirschsprung disease, acrocallosal syndrome, and congenital hydrocephalus (8). *L1CAM* mutations cause a wide variety of clinical phenotypes: hydrocephalus due to stenosis of the aqueduct of Sylvius (MIM #307000), MASA syndrome (mental retardation, aphasia, shuffling gait, adducted thumb; MIM #303350), and X-linked agenesis of the corpus callosum (MIM #217990). Phenotypic variability, even within a family, has been noted, raising the caution that definite clinical diagnosis in single

Table 1. Characterization of nucleotide changes found by exome sequencing

	FAM123B	*FRMD7*	*L1CAM*	*TMEM187*	*FLNA*	*LAGE3*
Change	c.85G>A (p.A29T)	c.875T>C (p.L292P)	c.92T>C (p.V31A)	c.334G>A (p.A112T)	c.1582G>A (p.V528M)	c.395G>A (p.R132Q)
PolyPhen	Benign	Probably damaging	Benign	Benign	Possibly damaging	Benign
PolyPhen-2	Probably damaging	Probably damaging	Benign	Possibly damaging	Possibly damaging	Possibly damaging
SIFT	0.04	0.02	0.22	0.02	0.04	0.46
MutationTaster	Polymorphism	Disease causing	Disease causing	Polymorphism	Polymorphism	Polymorphism
Normal female	8/502[a]	2/502	2/502	1/502	15/502[a]	4/502
Normal male	1/118	0/117	0/118	0/118		1/86
Note		No nystagmus in II-2				

[a]Including one homozygous female. Underlining means that this result excludes the variant as potentially causative. Grayed shading indicates the variants that could not be excluded; between these two, the *L1CAM* variant is more likely to be causative.

cases is often impossible (9). Phenotypic features compatible with the *L1CAM* mutation in our patients include spastic paralysis, aphasia, severe mental and growth retardation, but atypical leukodystrophy and the absence of adducted thumbs were very rare or exceptional (9). A normal control study found that 2 of 251 normal females were heterozygous for this SNP, but none of 117 normal males carried the variant allele. One of the four web-based analyses of pathological significance (MutationTaster) indicated that this variant would be disease causing, while the others indicated that it would be benign (Table 1). X-linked hydrocephalus due to *L1CAM* mutations occurs in approximately 1/30 000 male births (10). Considering that the *L1CAM* mutation was found in 2/618 control alleles (0.32%), the change may be a rare polymorphism, a mutation causing lethality in the majority of affected males, or a mutation with low penetrance. Because we were unable to exclude this *L1CAM* change, its pathogenic status remains inconclusive.

We next examined c.85G>A in *FAM123B*, c.875T>C in *FRMD7*, c.1582G>A in *FLNA*, and c.395G>A in *LAGE3* in normal controls. The *FAM123B*, *FLNA*, and *LAGE3* variants were excluded as causative because a homozygous change was found in 1 of 251 female controls (*FAM123B* and *FLNA*) or a hemizygous change was found in 1 of 86 normal males (*LAGE3*). However, the thick calvarium in individuals II-1 and II-2 may be influenced by the *FAM123B* change, because it is causative for osteopathia striata with cranial sclerosis, an X-linked dominant disorder (MIM #300373) (11, 12). As the calvarium of the patients' mother having the heterozygous *FAM123B* change was not evaluated by CT, we could not confirm this possibility.

Only 2 of 251 control females carried the c.875T>C variant in *FRMD7* heterozygously, and none of 117 male controls carried this variant; thus, the pathogenicity of the *FMRD7* variant was inconclusive. Other *FRMD7* mutations cause X-linked congenital nystagmus 1 (MIM #310700) (13). However, the nystagmus found in individual II-1 was not observed in individual II-2, indicating that the variant in common between two brothers did not consistently cause nystagmus. Thus, it may not contribute to the phenotype in this family (Table 1).

We also evaluated the c.334G>A variant in *TMEM187*. Only 2 of 251 female controls carried this heterozygous change, and it was not found among 118 male controls. Two of the four programs (PolyPhen-2 and SIFT) indicated that it would be pathogenic. By Taqman assay, *TMEM187* was ubiquitously expressed in various fetal and adult tissues, including the brain (data not shown), leaving the effect of this mutation on the phenotype in these patients inconclusive (Table 1).

In conclusion, we found two possible but inconclusive variants in this family with two boys affected by atypical leukodystrophy. High-throughput technologies are clearly powerful to detect genomic changes, but evaluation of the data can be very difficult and should be performed cautiously. More knowledge of rare SNPs and mutations is absolutely necessary before any conclusions can be drawn.

Acknowledgements

We would like to thank the patients and their family members for their participation in this study. This work was supported by research grants from the Ministry of Health, Labour and Welfare

(to H. S., N. Miyake, and N. Matsumoto), the Japan Science and Technology Agency (to N. Matsumoto), a Grant-in-Aid for Scientific Research from the Japan Society for the Promotion of Science (to N. Matsumoto), and a Grant-in-Aid for Young Scientists from the Japan Society for the Promotion of Science (to H. D., N. Miyake, and H. S.).

References

1. Saitsu H, Kato M, Mizuguchi T et al. De novo mutations in the gene encoding STXBP1 (MUNC18-1) cause early infantile epileptic encephalopathy. Nat Genet 2008: 40: 782–788.
2. Check Hayden E. Genomics shifts focus to rare diseases. Nature 2009: 461: 458.
3. Biesecker LG. Exome sequencing makes medical genomics a reality. Nat Genet 2010: 42: 13–14.
4. Kuhlenbaumer G, Hullmann J, Appenzeller S. Novel genomic techniques open new avenues in the analysis of monogenic disorders. Hum Mutat 2011: 32: 144–151.
5. Miyake N, Kosho T, Mizumoto S et al. Loss-of-function mutations of CHST14 in a new type of Ehlers-Danlos syndrome. Hum Mutat 2010: 31: 966–974.
6. Ng SB, Bigham AW, Buckingham KJ et al. Exome sequencing identifies MLL2 mutations as a cause of Kabuki syndrome. Nat Genet 2010: 42: 790–793.
7. Li H, Ruan J, Durbin R. Mapping short DNA sequencing reads and calling variants using mapping quality scores. Genome Res 2008: 18: 1851–1858.
8. Nakakimura S, Sasaki F, Okada T et al. Hirschsprung's disease, acrocallosal syndrome, and congenital hydrocephalus: report of 2 patients and literature review. J Pediatr Surg 2008: 43: E13–E17.
9. Rietschel M, Friedl W, Uhlhaas S, Neugebauer M, Heimann D, Zerres K. MASA syndrome: clinical variability and linkage analysis. Am J Med Genet 1991: 41: 10–14.
10. Rosenthal A, Jouet M, Kenwrick S. Aberrant splicing of neural cell adhesion molecule L1 mRNA in a family with X-linked hydrocephalus. Nat Genet 1992: 2: 107–112.
11. Viot G, Lacombe D, David A et al. Osteopathia striata cranial sclerosis: non-random X-inactivation suggestive of X-linked dominant inheritance. Am J Med Genet 2002: 107: 1–4.
12. Jenkins ZA, van Kogelenberg M, Morgan T et al. Germline mutations in WTX cause a sclerosing skeletal dysplasia but do not predispose to tumorigenesis. Nat Genet 2009: 41: 95–100.
13. Tarpey P, Thomas S, Sarvananthan N et al. Mutations in FRMD7, a newly identified member of the FERM family, cause X-linked idiopathic congenital nystagmus. Nat Genet 2006: 38: 1242–1244.

CLINICAL GENETICS An International Journal of Genetics, Molecular and Personalized Medicine

Clin Genet 2011: 80: 466–471
Printed in Singapore. All rights reserved

CLINICAL GENETICS
doi: 10.1111/j.1399-0004.2010.01554.x

Short Report

Familial Simpson–Golabi–Behmel syndrome: studies of X-chromosome inactivation and clinical phenotypes in two female individuals with *GPC3* mutations

Yano S, Baskin B, Bagheri A, Watanabe Y, Moseley K, Nishimura A, Matsumoto N, Ray PN. Familial Simpson–Golabi–Behmel syndrome: studies of X-chromosome inactivation and clinical phenotypes in two female individuals with *GPC3* mutations.
Clin Genet 2011: 80: 466–471. © John Wiley & Sons A/S, 2010

Simpson–Golabi–Behmel syndrome (SGBS) is an overgrowth/multiple congenital anomalies syndrome with an X-linked inheritance. Most cases of SGBS are attributed to mutations in the glypican 3-gene (*GPC3*), which is highly expressed in the mesodermal embryonic tissues and involves in a local growth regulation. Typical clinical features include pre/postnatal overgrowth, developmental delay, macrocephaly, characteristic facies with prominent eyes and macroglossia, diaphragmatic hernia, congenital heart defects, kidney anomalies, and skeletal anomalies. Obligate carrier females with *GPC3* mutations are usually asymptomatic or with mild symptoms. It is thought that skewed X-inactivation is the underlining mechanism for the female patients to present with findings of SGBS. We identified three siblings with typical SGBS (two male and one female cases) and their mother with very mild symptoms in a family carrying c.256C>T (p.Arg86X) mutation in *GPC3*. X-inactivation studies on the androgen-receptor gene (*AR*) and the Fragile XE (FRAXE) gene were performed with blood, buccal swabs, and fibroblasts in the carrier females. The studies with blood showed moderately skewed X-inactivation with paternal X-chromosome being preferentially inactivated (71–80% inactivated) in the female patient with SGBS and no skewing was shown in the mother with very mild symptoms. The X-inactivation studies in the mother showed inactivation of the X-chromosome with the mutation by 57%. This suggests that loss of the functional GPC3 protein by 43% is closed to the threshold to develop the SGBS phenotype. Studies with buccal swabs and fibroblasts failed to show different X-inactivation patterns between the two female individuals.

Conflict of interest

Nothing to declare.

S Yano[a], B Baskin[b], A Bagheri[a], Y Watanabe[c], K Moseley[a], A Nishimura[d], N Matsumoto[d] and PN Ray[b]

[a]Genetics Division, Department of Pediatrics, LAC+USC Medical Center, Keck School of Medicine, University of Southern California, Los Angeles, CA, USA, [b]Division of Molecular Genetics, Department of Pediatric Laboratory Medicine, The Hospital for Sick Children, Toronto, ON, Canada, [c]Department of Pediatrics and Child Health, Kurume University School of Medicine, Kurume, Japan, and [d]Department of Human Genetics, Yokohama City University Graduate School of Medicine, Yokohama, Japan

Key words: buccal swabs – GPC3 – skewed X-chromosome inactivation – SGBS – skin fibroblasts

Corresponding author: Shoji Yano, Genetics Division, Department of Pediatrics, LAC+USC Medical Center, Keck School of Medicine, University of Southern California, Los Angeles, CA, USA.
Tel.: +1-323-226-3816;
fax: +1-323-226-6073;
e-mail: syano@usc.edu

Received 24 July 2010, revised and accepted for publication 20 September 2010

Introduction

Simpson–Golabi–Behmel syndrome (SGBS) is an X-linked overgrowth syndrome characterized by pre- and postnatal macrosomia, macrocephaly, characteristic facies including hypertelorism, macrostomia, macroglossia, mental retardation, and other variable anomalies including congenital diaphragmatic hernia, congenital heart defects, renal defects, gastrointestinal anomalies, and skeletal anomalies including vertebral fusion, scoliosis, pectus excavatum, and rib anomalies (1–5). An incidence of neoplasia is reported to be approximately 10% in patients with SGBS (6). The glypican 3 (*GPC3*) gene is the only gene known to cause SGBS, although a severe variant form has recently been mapped to Xp22 (7, 8). *GPC3* is located at Xq26 and encodes the glypican-3 protein which is a glycosylphosphatidylinositol-linked cell surface heparan sulfate proteoglycan. It is thought to play an important role in growth control in embryonic mesoderm derived tissues (7). SGBS has a wide range of clinical manifestations and genotype–phenotype correlations have not been recognized (7, 9). Mutations in *GPC3* causing SGBS are believed to result in a loss-of-function of the glypican-3 protein (10). Although, carrier females can have mild manifestations of SGBS, they do not usually have typical clinical features of SGBS (2, 11). A female with typical SGBS with an X-autosome translocation has been reported (12). These observations likely suggest that skewed X-inactivation is the underlining mechanism for wide clinical phenotypic manifestations in female carriers with *GLP3* mutations.

Aims of the study

The aim of the study was to evaluate if skewed X-chromosome inactivation was responsible for female patients with *GPC3* mutations to develop clinical features of SGBS.

Subjects and methods

Subjects 1, 2 and 3 are Jordanian siblings from non-consanguineous healthy parents (Fig. 1). Subjects 1 and 2 are male, while subject 3 is female. Subjects 2 and 3 are dizygotic twins. Pertinent clinical findings are summarized in the Table 1. Subject 1 was prenatally diagnosed with hydronephrosis, hydroureters, and polyhydramnios. He was delivered at 37 weeks by caesarian section because of macrosomia and weighed 3920 g. A diagnosis of SGBS was suspected in the neonatal period because of prenatal onset of overgrowth and physical features including

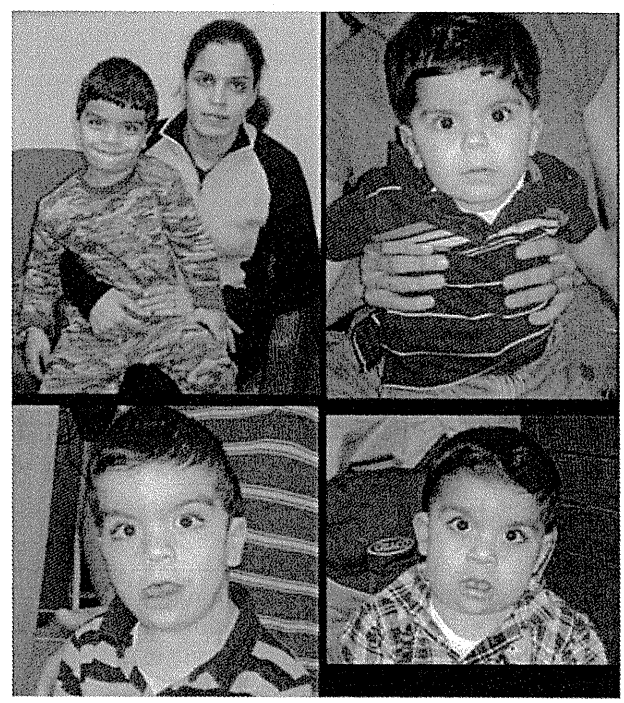

Fig. 1. Upper left: photos of Subject 1 (30 months) and Subject 4 (26 years); Upper right: photo of Subject 3 (12 months); Lower left: photo of Subject 1 (25 months); Lower right: photo of Subject 2 (12 months).

down-slanting palpebral fissures, prominent ala nasi, prominent metopic suture, macroglossia, mild pectus excavatum, large feet and hands and skeletal anomalies with 13 ribs. DNA sequence analyses of *GPC3* revealed a mutation of c.256C>T (p.Arg86X) confirming the diagnosis. His motor and speech development have been delayed: walking at 15 months and <10 words vocabulary at 25 months. Subject 2 was born at 34 weeks gestation by caesarian section. He weighed 3710 g (>97th percentile on the adjusted preterm growth chart). He was also diagnosed prenatally with hydronephrosis, hydroureters, and macrocephaly/macrosomia, and skeletal survey at birth showed abnormal chest cage with 13 ribs. At 3 months of age, he had mild scaphocephaly, characteristic facies with proptotic and prominent eyes, prominent ala nasi and up-turned nose and mild pectus excavatum. X-ray studies at 12 months showed advanced bone age equivalent to 16 months. His development has been delayed: he could not walk independently and had four single words at 17 months. The same mutation of c.256C>T (p.Arg86X) was identified in *GPC3*. Subject 3 is a female, the dizygotic twin sister of subject 2. She weighed 2196 g at birth (below the 50th percentile for weight). She was diagnosed with a congenital diaphragmatic hernia that was surgically repaired in the neonatal period.

Table 1. Summary of clinical findings

Sb. 1 Male	Sb. 2 Male	Sb. 3 Female	Sb. 4 Female	Clinical findings
(37 weeks)	(34 weeks)	(34 weeks)	FT	At birth (gestational age)
+	+	−		Macrosomia
3920 g	3710 g	2195 g	unk	Birth weight
−	−	−	−	Craniofacial
+	+	+	−	Macrocephaly
+	+	+	+ mild	Coarse face
+	+	−	−	Ocular hypertelorism
+	+	−	−	Epicanthal folds
+	+	−	−	Thick auricles
+	+	+	−	Wide nasal bridge and anteverted nares
+	+	−	+ mild	Macrostomia/macroglossia
+	+	−	−	Midline groove in the lower lip and/or deep furrow in the middle of the tongue
+	+	−	−	High arched/narrow palate
−	−	−	−	Hands
+	+	−	−	Large hands
−	−	−	−	Postaxial polydactyly
−	−	−	−	Chest/abdomen
−	−	−	−	Supernumerary nipples
+	+	−	−	Pectus excavatum
+	+	−	−	Rib/vertebral abnormalities
+	+	−	−	Umbilical/inguinal hernias
−	−	−	−	Genitalia
+	−			Hydrocele
−	−	−	−	Internal organs
+	−	+	−	Congenital heart defect
VSD	−	PDA	−	(VSD: ventricular septal defect, PDA: patent ductus arteriosus)
−	−	+	−	Diaphragmatic hernia
+	+	−	−	Hepatomegaly
−	−	+	−	Cystic dysplasia of kidneys
+	+	−	−	Nephromegaly
+	+	−	−	Hydronephrosis
−	+	−	−	Hydroureter
−	−	−	−	Neurological findings
+	+	−	−	Speech delay
+	+	+	−	Motor delay
−	−	−	−	Other findings
+	−	+	−	Vertebral anomalies
+	+	−	−	Advanced bone age

FT, full term; unk, unknown; Sb, subject; Sb2 and 3 are dizigotic twins.

Ultrasound studies showed a small patent ductus arteriosus (PDA) and small cystic lesions in the left kidney. She had a developmental evaluation at the age of 5 months which revealed fine motor delay. At the age of 3 months, her height, weight and occipito-frontal circumference were at the 10th, 25th, and 25th percentile, respectively. However, by 8 months of age all the measurements were above the 90th percentile. Although, her facial features were not typical for SGBS, developmental delay and dysmorphic features including macrocephaly, PDA and congenital diaphragmatic hernia strongly suggested SGBS. Subject 4 is their mother. She has normal intelligence, and is in good health. She has very mild clinical signs such as slight coarse facies and macrostomia. Subjects 3 and 4 were tested for *GPC3* mutations, which revealed the heterozygous mutation of c.256C>T (p.Arg86X).

Methods

Assays for the analyses of X-chromosome inactivation were performed using genomic DNA extracted from peripheral blood, buccal swabs, and cultured skin fibroblasts in the two female

individuals with the mutation in *GPC3*. The X-chromosome inactivation status was evaluated by the following two methods: the analysis of the CAG repeats in the human androgen-receptor gene (*AR*) at Xq11-q12 following the method described by Allen et al. (13) and the analysis of the CCG repeats in the 5′-untranslated region of the Fragile XE (*FRAXE*) gene at Xq28 using forward: 5′-GCGAGGAAGCGGCGGCAGTGGCACTGGG-3′ and reverse: 5′-CCTGTGAGTGTGTAAGTGT GTGATGCTGCCG-3′ primers following the same protocol as above. [University of Southern California Health Science Campus Institutional Review Board approved (ethics approval) the study.]

Results

Analysis of *AR* indicated that the mother had homozygous alleles with 21 CAG repeats and subject 3 received an X-chromosome containing the 21 CAG repeats allele from the mother and the 22 repeats allele from the father. The studies in subject 3 revealed that the X-inactivation ratio was 21 (20%) : 22 (80%).

The result indicates that paternal X-chromosome ($n = 22$ repeats) was preferentially inactivated in subject 3 and the studies were not informative for the mother. Analysis of *FRAXE* indicated that the mother had an allele with 14 (CCG) repeats and an allele with 20 repeats. The X-inactivation ratio was 14 (57%) : 20 (43%). Subject 3 received an allele with 14 repeats from the mother and the other with 17 repeats from the father. The X-inactivation ratio was 14 (29%) : 17 (71%). This indicates that the X-chromosome with the mutation was inactivated by 57% in the mother (subject 4) and by 29% in her affected daughter (subject 3). The study results with buccal swabs and cultured skin fibroblasts specimens were quite different from the ones with blood specimens (Table 2). Analysis of *AR* with skin fibroblasts showed that the X-inactivation ratio was 21 (72%) : 22 (28%) in subject 3. Analysis of *FRAXE* with skin fibroblasts showed the ratio of 14 (77%) : 17 (23%) in subject 3 and 14 (70%) : 20 (30%) in subject 4. Analysis of FRAXE with buccal swabs specimens showed the ratio of 14 (44%) : 17 (56%) in subject 3 and 14 (42%) : 20 (58%) in subject 4.

Table 2. Analysis of X-inactivation by the androgen receptor (*AR*) and the fragile XE (*FRAXE*) loci

Gene	Specimen	Subject 3		Subject 4	
AR	(Repeats)	(21)	(22)	(21)	(21)
	Blood, $n = 2$	20	80	n/a	n/a
	Fibroblasts, $n = 2$	72	28	n/a	n/a
FRAXE	(Repeats)	(14)	(17)	(14)	(20)
	Blood, $n = 3$	29	71	57	43
		SD: 2		SD: 3.6	
	Fibroblasts, $n = 3$	77	23	70	30
		SD: 1		SD: 8.4	
	Buccal swabs	44	56	42	58

Subject 4 was homozygous for the repeats at *AR*.
n, number of repeated assay; n/a, not applicable; SD, standard deviation.

Discussion

SGBS is an X-linked condition and mutations in *GPC3* at Xq26 are known to be responsible to cause SGBS (7). *GPC3* encodes the glypican-3 protein which is thought to play an important role in growth control in embryonic mesoderm derived tissues (7). Although, *GPC3* is highly expressed in mesodermal embryonic tissues including liver, lung, and kidney, it is expressed neither in the fetal brain tissue nor in skin fibroblasts as they are formed from the ectoderm. The studies were conducted with blood, buccal swabs and skin fibroblasts. Only the studies with blood cells could show moderately skewed X-inactivation in the affected daughter (subject 3) with the ratio of inactivation of the X-chromosome without the mutation by 71–80%. Her mother with mild symptoms (subject 4) did not show skewed X-inactivation with blood specimens. As *GPC3* has tissue specific expressions and is not one of the housekeeping genes, it is not expressed in the ectodermal cells. Skin fibroblasts and buccal swabs may not be suitable specimens to study the effects of *GPC3* mutation because of skewed X-inactivation. Blood cells and internal organs including lung, liver and kidney are formed from the mesoderm. Although, *GPC3* is minimally expressed in adult tissues, the profile of X-inactivation should remain the same from the embryo stage (7). As analyses of X-inactivation with internal organs are impractical, blood is likely the most appropriate specimen that possibly reflects abnormal *GPC3* functions at embryonic stage because of skewed X-inactivation.

X-linked disorders affect males, where as female carriers are generally spared. This is thought to be because of the random inactivation in females of one of the two X-chromosomes in all somatic cells (14). Only a few female patients with mild expressions of the SGBS phenotype have been reported (2, 11). A female with typical SGBS with an X-autosome translocation has been reported by Punnett (12). An X-autosome translocation is known to cause skewing effects because of the selection for survival advantage (15). Approximately 10% of the population

shows skewing as extreme as 90/10 by random X-inactivation (16). On the basis of these observations, it is thought that the effect of Lyonization is the underlining mechanism for female carriers to have a milder phenotype. The X-chromosome inactivation studies in the presented family showed that predominant expression of the X-chromosome with the *GPC3* mutation in subject 3 and predominant expression of the normal X-chromosome in the mother with mild symptoms (Subject 4). It is unclear why there is 9% difference between the two results with *AR* and *FRAXE* in subject 3. This might be reflecting the limitations of accuracy in these X-inactivation studies. Skewed X-inactivation usually means that an allele is preferentially inactivated by >90% (17). As it does not seem to be survival advantage over the cells without the mutation in GPC3, moderate degree of skewed X-inactivation in the subject 3 is likely because of random X-inactivation. The mechanisms leading to a skewed X-inactivation in females with X-linked disorders are reviewed by Puck and Willard (14).

Discordant expression of a few housekeeping genes including hypoxanthine guanine phosphoribosyltransferase (HPRT, EC 2.4.2.8) and alpha-galactosidase A (EC 3.2.1.22) in monozygotic twin pairs with Lesch–Nyhan disease and with Fabry disease, respectively, have been reported (18, 19). In these reports, X-inactivation analyses showed different patterns between blood cells and skin fibroblasts. A skewed pattern was demonstrated in the fibroblasts in the affected twins in these conditions. Although, a hypothesis that the process responsible for monozygotic twinning to lead skewed X-inactivation in monozygous twin sisters may exist, it is probably unlikely for the process to affect the moderately skewed X-inactivation of blood cells in the affected dizygotic twin female subject (subject 3) as chromosome studies with her blood did not show a chimera with 46,XY cells (18). Placental vascular connections occur in 8% of dizygotic twins (20). However, it is unlikely that vascular connections could have any effects on the profile of X-inactivation in subject 3.

In the presented case here, subject 3 showed a moderately skewed X-inactivation (71–80%). Loss of the functional glypican-3 protein by 71–80% degree is appeared to be above the threshold to develop the SGBS phenotype. The X-inactivation studies in the mother showed inactivation of the X-chromosome with the mutation by 57%. This suggests that loss of the functional glypican-3 protein by 43% is slightly above or close to the threshold to develop the SGBS phenotype.

These X-inactivation studies with peripheral blood DNA specimens (mesoderm origin) showed the most reasonable results that can provide explanations for the phenotypic features in the two female subjects. Ectodermal origin of skin fibroblasts and buccal swabs showed the contradicting results against the ones from blood specimens and the two female subjects showed the almost identical X-inactivation patterns. This suggests that it is critical to choose appropriate specimens based on the gene functions and expressions to evaluate if skewed X-inactivation is responsible for clinical findings. Further studies are indicated to disclose correlation of *GPC3* genotypes, the levels of expression, and clinical phenotypes in female individuals with SGBS.

References

1. Simpson JL, Landey S, New M et al. A previously unrecognized X-linked syndrome of dysmorphia. Birth Defects 1975: 11: 18–24.
2. Golabi M, Rosen L. A new X-linked mental retardation overgrowth syndrome? Am J Med Genet 1984: 17: 345–358.
3. Behmel A, Plochi E, Rosenkranz W. A new X-linked dysplasia gigantism syndrome: identical with the Simpson dysplasia syndrome? Hum Genet 1984: 67: 409–413.
4. Neri G, Marini R, Cappa M et al. Simpson-Golabi-Behmel syndrome: an X-linked encephalo-tropho-schisis syndrome. Am J Med Genet 1988: 30: 287–299.
5. Chen E, Johnson JP, Cox VA et al. Simpson-Golabi-Behmel syndrome: Congenital diaphragmatic hernia and radiologic findings in two patients and follow-up of a previously reported case. Am J Med Genet 1993: 46: 574–578.
6. Li M, Shuman C, Fei YL et al. GPC3 mutation analysis in a spectrum of patients with overgrowth expands the phenotype of Simpson-Golabi-Behmel syndrome. Am J Med Genet 2001: 102: 161–168.
7. Pilia G, Hughes-Benzie RM, Mackenzie A et al. Mutations in GPC3, a glypican gene, cause the Simpson-Golabi-Behmel syndrome. Nat Genet 1996: 12: 241–247.
8. Brzustowicz LM, Farrell S, Khan MB et al. Mapping of a new SGBS locus to chromosome Xp22 in a family with a severe form of Simpson-Golabi-Behmel syndrome. Am J Hum Genet 1999: 65: 779–783.
9. Mariane S, Iughetti L, Bertorelli R et al. Genotype/phenotype correlations of males affected by Simpson-Golabi-Behmel syndrome with GPC3 gene mutations: patient report and review of the literature. J Pediatr Endocrinol Metab 2003: 16: 225–232.
10. Veugelers M, Cat BD, Muyldermans SY et al. Mutation analysis of the GPC3/GPC4 glypican gene cluster on Xq26 in patients with Simpson-Golabi-Behmel syndrome: identification of loss-of-function mutations in the GPC3 gene. Hum Mol Genet 2000: 9: 1321–1328.
11. Behmel A, Plochl E, Rosenkranz W. A new X-linked dysplasia gigantism syndrome: follow up in the first family and report on a second Austrian family. Am J Med Genet 1988: 30: 275–285.
12. Punnett HH. Simpson-Golabi-Behmel Syndrome in a female with an X-autosome translocation. Am J Med Genet 1994: 50: 391–393.
13. Allen RC, Zoghbi HY, Moseley AB et al. Methylation of *Hpa*II and *Hha*I sites near the polymorphic CAG repeat in the

human androgen-receptor gene correlates with X chromosome inactivation. Am J Hum Genet 1992: 51: 1229–1239.
14. Puck JM, Willard HF. X inactivation in females with X-linked disease. N Engl J Med 1998: 338: 325–328.
15. Heard E, Clerc P, Avner P. X chromosome inactivation in mammals. Annu Rev Genet 1997: 31: 571–610.
16. Naumova AK, Plenge RM, Bird LM et al. Heritability of X chromosome inactivation phenotypes in a large family. Am J Hum Genet 1996: 58: 1111–1119.
17. Beever CL, Stephenson MD, Penaherrera MS et al. Skewed X-chromosome inactivation is associated with trisomy in women ascertained on the basis of recurrent spontaneous abortion or chromosomally abnormal pregnancies. Am J Hum Genet 2003: 72: 399–407.
18. De Gregorio L, Jinnah HA, Harris JC et al. Lesch-Nyhan disease in a female with a clinically normal monozygotic twin. Mol Genet Metab 2005: 85: 70–77.
19. Redonnet-Vernhet I, van Amstel JKP, Jansen RPM et al. Uneven X inactivation in a female monozygotic twin pair with Fabry disease and discordant expression of a novel mutation in the alpha-galactosidase A gene. J Med Genet 1996: 33: 682–688.
20. Hall JG. Twinning: mechanism and genetic implications. Curr Opin Genet Dev 1996: 6: 343–347.